equivalent atoms in other substitutions ($C^{\gamma 2}$ of Leu^{129} and $C^{\gamma 2}$ of Ile^{149}) (*21*).

33. The T4 lysozyme gene was amplified with polymerase chain reaction (PCR) with the use of degenerate primers encoding all 20 amino acids and one stop codon (X, X, G or T, where X is A, T, G, or C) at the target sites (*9*). Three overlapping fragments bounded by the mutagenesis sites and the gene termini were generated and subsequently linked together with PCR in two steps. The full-length mutagenized gene fragment was cut with restriction enzymes and ligated into an engineered bacteriophage λ selection vector (*9*) that relied on the activity of the cloned T4 lysozyme gene to complement a defect in its own homologous lysis (R) gene (*25*). Plaque-forming phages were isolated and functional T4 lysozyme genes were excised as part of a phagemid for both protein expression and DNA sequencing (*26*). A plate assay (*27*) was used to sort the variants into rough categories of stability and activity. A total of 106 new amino acid combinations were obtained at a frequency of 10^{-2} from the screening of 25,000 phages, and a number of these were chosen for crystallographic and thermodynamic analysis. Protein preparation (*27*), thermal denaturation at pH 3 (*10*), and crystal growth (*3*) were as described. Data from x-ray measurements were collected (*28*), and structures were refined (*29*) starting with the cysteine-free wt model (*30*). No torsion angle restraints were imposed during refinement. Final models have deviations from ideal geometry less than or equal to 0.015 Å (bond lengths) and 2.1° (bond angles).

34. We thank J. H. Hurley, X.-J. Zhang, and A. R. Poteete for helpful discussions and S. Pepiot, J. Xu, and N. Gassner for help with the purification and analysis of various mutant lysozymes. Supported by a National Institutes of Health postdoctoral fellowship (GM12989) (E.P.B.) and grant (GM21967) (B.W.M.).

29 June 1993; accepted 19 October 1993

Modulation of Calmodulin Plasticity in Molecular Recognition on the Basis of X-ray Structures

William E. Meador, Anthony R. Means, Florante A. Quiocho*

Calmodulin is the primary calcium-dependent signal transducer and regulator of a wide variety of essential cellular functions. The structure of calcium-calmodulin bound to the peptide corresponding to the calmodulin-binding domain of brain calmodulin-dependent protein kinase IIα was determined to 2 angstrom resolution. A comparison to two other calcium-calmodulin structures reveals how the central helix unwinds in order to position the two domains optimally in the recognition of different target enzymes and clarifies the role of calcium in maintaining recognition-competent domain structures.

Calmodulin (CaM) exerts its role by activating more than 20 different enzymes in eukaryotic cells. Studies in solution show that the helical content of CaM is increased upon binding Ca^{2+} (*1*). The next step in the mechanism of signal transduction requires binding of Ca^{2+}-CaM to an acceptor protein. Much of what is known about such physical interactions comes from the use of synthetic peptides corresponding to the CaM-binding domains of various physiologically relevant target proteins or enzymes and also peptide drugs and toxins (*2*). Often these peptides have very little sequence similarity (Fig. 1). Calcium-CaM bound to these peptides [dissociation constant values in the nanomolar range (*2, 3*)] has been shown especially by physical techniques to be considerably more compact than the unbound form, which indicates the extraordinary flexibility of CaM (*4*). These observations led to suggestions that in the Ca^{2+}-CaM-peptide ternary complex the two domains of Ca^{2+}-CaM interact simultaneously with opposite ends of the peptide (*2, 4*). The x-ray structures of native Ca^{2+}-CaM show that the two domains, each containing a pair of Ca^{2+} atoms, are widely separated by a seven-turn central or linker helix with an unusually high thermal motion (*5–7*). The three-dimensional structure determinations of Ca^{2+}-CaM bound to synthetic peptide analogs of the CaM-binding regions of skeletal and smooth muscle myosin light chain kinase by nuclear magnetic resonance (*8*) and x-ray crystallography (*9*), respectively, have revealed that a portion of the central helix in the unbound structure uncoiled, enabling the two domains to engulf the helical target peptides. The mode of binding of the regulatory light chain seen recently in the S1 myosin crystal structure (*10*) has features that resemble those of the bound Ca^{2+}-CaM structures.

Our report focuses on the detailed structural basis for the ability of CaM to recognize the different targets and initiate signal transduction. We report the refined 2 Å structure of the complex of Ca^{2+}-CaM with the CaM-binding domain peptide (Fig. 1) of the brain CaM-dependent protein kinase IIα (CaMKII) (Fig. 2) and compare it to the 1.7 Å structure of Ca^{2+}-CaM (*7*) and the 2.4 Å structure of the complex with the different peptide from smooth muscle myosin light chain kinase (smMLCK) (*9*), which has been further refined at 2.2 Å (*11*). Whereas the smMLCK peptide is observed in its entirety in the electron density of the refined complex structure (*9*), only residues 293 to 310 of the CaMKII peptide show density and make contacts of 4 Å or less with Ca^{2+}-CaM (Figs. 2 and 3, A and B). The ordered segments define more closely the CaM-binding domain of the target enzymes within the context of the peptide fragments.

As can be seen in Figs. 2B and 3A, the ellipsoidal compact structure of Ca^{2+}-CaM bound to the CaMKII peptide bears some resemblance to that bound to the smMLCK peptide (*9*). The two domains of Ca^{2+}-CaM (identified as NH_2- and COOH-domains or lobes) wrapped around and engulfed the target peptide. The two domains approach in the central latch region (between helices II and VI) to again create a pseudo twofold symmetry and a continuous hydrophobic arc, formed from the coalescing of the wide hydrophobic patches in both domains, that apposes the hydrophobic side of the helical peptide. The NH_2- and COOH-terminal halves of the CaMKII peptide interact mainly with the COOH- and NH_2-domains of Ca^{2+}-CaM, respectively, with the exception of the consecutive basic side chains (Arg^{296}-Arg^{297}-Lys^{298}) in the NH_2-terminus, which make hydrogen bonding and salt-linking interactions with glutamate residues on both domains. Aiding maximal contact of the Ca^{2+}-CaM lobes with the target peptide, a portion of the central helix in the native Ca^{2+}-CaM structure again is pulled out into a strand (Fig. 3C), which we have referred to earlier as the "expansion joint" to underscore this unique and functionally critical region of CaM (*9*).

Consistent in part with previous general suggestions [summarized in (*2*)], a major determinant in molecular recognition appears to be the hydrophobic interactions between the shallow hydrophobic pockets in the two domains of Ca^{2+}-CaM and specific hydrophobic residues of target peptides. As can be seen in Figs. 2B and 3A, the pocket in the COOH-domain harbors Leu^{299} of the CaMKII peptide or its coun-

CaMKII peptide (residues 290 to 314)	LKKFNARRKLKGAILTTMLATRNFS
smMLCK peptide (residues 796 to 815)	ARRKWQKTGHAVRAIGRLSS

Fig. 1. Peptide segments corresponding to the CaM-binding domains of CaMKII and smMLCK used in the x-ray studies (*17*). The alignment of the peptide sequences is based primarily on an almost total identity between residues 295 to 299 of the CaMKII peptide and residues 796 to 800 of the smMLCK peptide (Fig. 3, A and B).

W. E. Meador and F. A. Quiocho, Howard Hughes Medical Institute and Departments of Biochemistry and Molecular Physiology and Biophysics, Baylor College of Medicine, Houston, TX 77030.
A. R. Means, Department of Pharmacology, Duke University Medical School, Durham, NC 27710.

*To whom correspondence should be addressed.

terpart Trp^{800} of the smMLCK peptide found near the NH_2-terminal end, and the similar pocket in the NH_2-domain contains Leu^{308} near the middle of the CaMKII peptide or Leu^{813} close to the COOH-terminal end of the smMLCK peptide.

The electrostatic interactions have a focus at the NH_2-terminus of the CaMKII and smMLCK peptides, where there is a cluster of basic residues (Figs. 1, 2B, and 3B), a motif present in a number of CaM-binding domains that bind with nanomolar affinity (*2*, *3*). Because this positive charge cluster is flanked by two glutamate clusters of Ca^{2+}-CaM in both bound structures and interacts extensively with them, it is evident that a role exists for these electrostatic interactions in orienting CaM binding in the recognition process.

The geometry of binding and specific interactions of the two domains of Ca^{2+}-CaM are influenced by the target sequences. In this comparison (Fig. 3A), the changes are more apparent with the interaction involving the NH_2-lobe. In the COOH-terminal portion of the peptides, a number of sequence differences between the CaMKII and smMLCK peptides resulted in geometrical and contact changes in the binding of the NH_2-domain. The motif of two aliphatic long chain or aromatic residues separated by 12 residues found in many CaM-binding sequences (that is, Trp^{800} and Leu^{813} in the smMLCK peptide) is not observed in the CaMKII peptide (Fig. 1). The Leu^{299} residue of the CaMKII peptide (as well as Ile^{303}) is inserted in the same hydrophobic patch as its homolog Trp^{800} of the smMLCK peptide, but the interaction of Leu^{813} of the smMLCK peptide does not mirror that of its counterpart Asn^{312} of the CaMKII peptide, which is disordered in the structure. Instead, the NH_2-domain moved with respect to its position in the structure of the complex with the smMLCK peptide in order to accommodate Leu^{308} of the CaMKII peptide in the hydrophobic patch. Further aided by the replacement of a bulky Ile^{810} in the smMLCK peptide with an Ala^{309} in the CaMKII peptide and the removal of a steric hindrance by Lys^{802} in the smMLCK peptide with Gly^{301} in the CaMKII peptide, the movement of the NH_2-domain as a whole is a tilt toward the NH_2-terminus of the peptide, with a slight intradomain shift of helix I toward helix IV.

The binding of the COOH-lobe is similar in the two Ca^{2+}-CaM peptide structures in spite of some sequence differences in the NH_2-terminal half of the two peptides. For example, although the counterpart of Ile^{303} in the CaMKII peptide is Gly^{804} in the smMLCK peptide, the COOH-domain, which mainly interacts with this portion of the peptide, seems to have accommodated the bulky Ile side chain with a minimum of adjustment relative to the complex with the smMLCK peptide, which shows only a modest rotation about the peptide and a slight outward movement of the COOH-terminal helix (VIII) of Ca^{2+}-CaM.

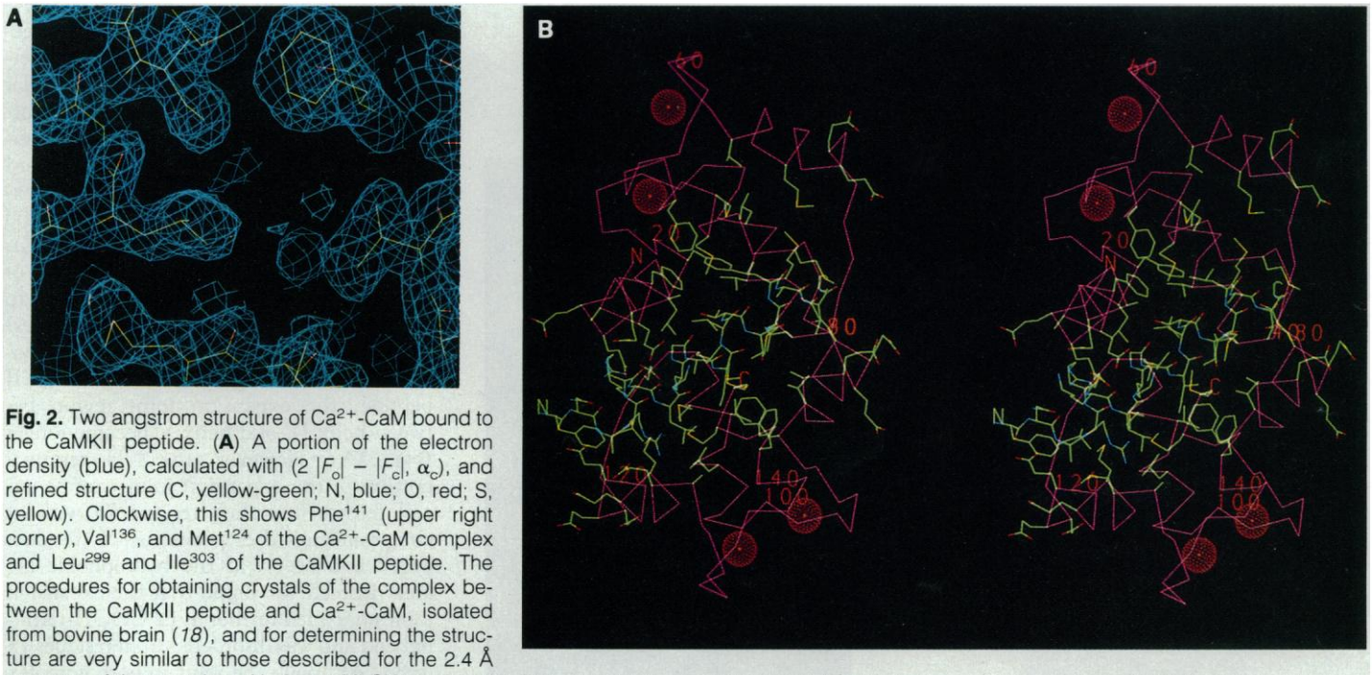

Fig. 2. Two angstrom structure of Ca^{2+}-CaM bound to the CaMKII peptide. (**A**) A portion of the electron density (blue), calculated with $(2|F_o| - |F_c|, \alpha_c)$, and refined structure (C, yellow-green; N, blue; O, red; S, yellow). Clockwise, this shows Phe^{141} (upper right corner), Val^{136}, and Met^{124} of the Ca^{2+}-CaM complex and Leu^{299} and Ile^{303} of the CaMKII peptide. The procedures for obtaining crystals of the complex between the CaMKII peptide and Ca^{2+}-CaM, isolated from bovine brain (*18*), and for determining the structure are very similar to those described for the 2.4 Å structure of the complex with the smMLCK peptide (*9*). The crystal form of the Ca^{2+}-CaM-CaMKII peptide complex, which is different from that of the complex with the smMLCK peptide (*9*), belongs to space group $C222_1$ with unit cell dimensions of $a = 39.00$ Å, $b = 75.20$ Å, and $c = 120.15$ Å and one molecule of CaM peptide complex in the asymmetric unit. The phases were determined by the single isomorphous replacement–anomalous dispersion technique, with $Pb(NO_2)_2$ as the heavy atom derivative. A 3.5 Å electron density map calculated with the heavy-atom phases (mean figure of merit of 0.57) was good enough to initially fit the two domains of Ca^{2+}-CaM, each separately as a rigid body, and a portion of the CaMKII peptide. The model of the Ca^{2+}-CaM-CaMKII peptide complex was refined with the X-PLOR suite of programs (*19*). The final *R* factor is 0.208 for 9535 reflections between 10.0 to 2.0 Å resolution. The refined structure has good geometry, with a root-mean-square deviation from ideality of 0.011 Å for distances and 1.28° for angles. The program CHAIN (*20*) was used in fitting the model to electron density maps and molecular graphics analysis of the structure. (**B**) Stereo view of the α carbon backbone structure of Ca^{2+}-CaM (magenta) bound to the CaMKII peptide [all atoms with standard color as in (A)]. The four Ca^{2+} atoms are shown as spherical dot surfaces. The NH_2- and COOH-terminal ends of CaM and the peptide are identified by N and C, respectively. The Ca^{2+}-CaM residues displayed are the hydrophobic residues near the peptide analog and all glutamate residues excepting those near Ca^{2+}-binding sites. Glu residues 7, 11, 14, 114, and 127 belong to two large clusters of these residues (one on helix I and the other on helix VII) and make hydrogen bonds and salt links with the three consecutive basic residues near the NH_2-terminal end of the CaMKII peptide. The strand of residues 73 to 83, which divides the central helix of native Ca^{2+}-CaM into two helices (IV and V) in the bound form, has very little electron density in the refined structure, a reflection of very high mobility. The model of this strand (which is also shown in Fig. 3, A and C) is the result of simulated annealing and energy minimization in the course of the X-PLOR refinement. The first three and last two residues of Ca^{2+}-CaM and the first three and last four residues of the CaMKII peptide have no density and are not shown.

The critical element in the hydrophobic interactions is the presence of at least two hydrophobic residues in the CaM-binding segment separated by an 8- or 12-residue sequence (Figs. 1 and 3, A and B). Thus, the significance previously attached by other investigators (*2*, *8*, *12*) to a 12-residue sequence separating the hydrophobic residues near both ends of the segments observed in many CaM-binding domains (that is, those of smooth and skeletal muscle myosin light chain kinases) is only partially valid (*13*).

A total of 135 contacts of ≤4 Å are formed in the complex with the CaMKII peptide, about 40 less than with the smMLCK peptide (*9*). About 80% of all contacts in both complexes are van der Waals interactions, which accounts for the ability of Ca^{2+}-CaM to bind tightly to many target enzymes with CaM-binding domains that lack sequence similarity. Notably, all of the nine Met residues of Ca^{2+}-CaM (*2*, *14*), as well as several Phe, Leu, Val, and Ala residues, are in positions to participate in binding to target enzymes. Moreover, the extensive participation of glutamates of Ca^{2+}-CaM as almost the sole polar residues has not been heretofore recognized (Fig. 3B).

In comparing the structures of native Ca^{2+}-CaM and the two CaM peptide complexes, we find changes in the conformations of many side chains that make contact with the peptides, especially in the Glu and Met residues that have flexible side chains (*11*). Thus, there are local as well as global structural changes associated with molecular recognition. However, domain structures overall for the two target-bound forms are similar to those of the unbound form. It is noteworthy that the Ca^{2+}-binding sites in the unbound and bound structures of Ca^{2+}-CaM are distant from the peptides and are exposed, enabling unhindered access to and from these sites (Figs. 2B and 3, A and C).

How is it possible for the domains of Ca^{2+}-CaM to make the adjustments to accommodate different target sequences? Because of the nature of the domain disposition in the complex with the CaMKII peptide, the expansion joint region between helix IV and helix V became longer (Fig. 3A). However, the NH_2-terminal portion of the expansion joint cannot uncoil further preceding residue 73 without compromising the positions of residues Met^{71} and Met^{72} in the hydrophobic arc area. Instead, we found that the expansion joint unraveled further at its COOH-terminal end and was disordered from residues 73 to 83. Although the joint in both complex structures commences at residue 73, it terminates at residue 77 in the Ca^{2+}-CaM complex bound to the smMLCK peptide (*9*). Thus, the central helix of Ca^{2+}-CaM plays a key role by acting as a variable expansion joint, allowing different relative positionings of the lobes as different target enzymes are recognized. This role of a protein helix is novel (*15*).

Calmodulin in the Ca^{2+}-free form is less organized (*1*). However, 3D structures of Ca^{2+}-CaM bound to its target as well as unbound show similarity and hence some rigidity in the domain structures, but also show high thermal parameters and hence

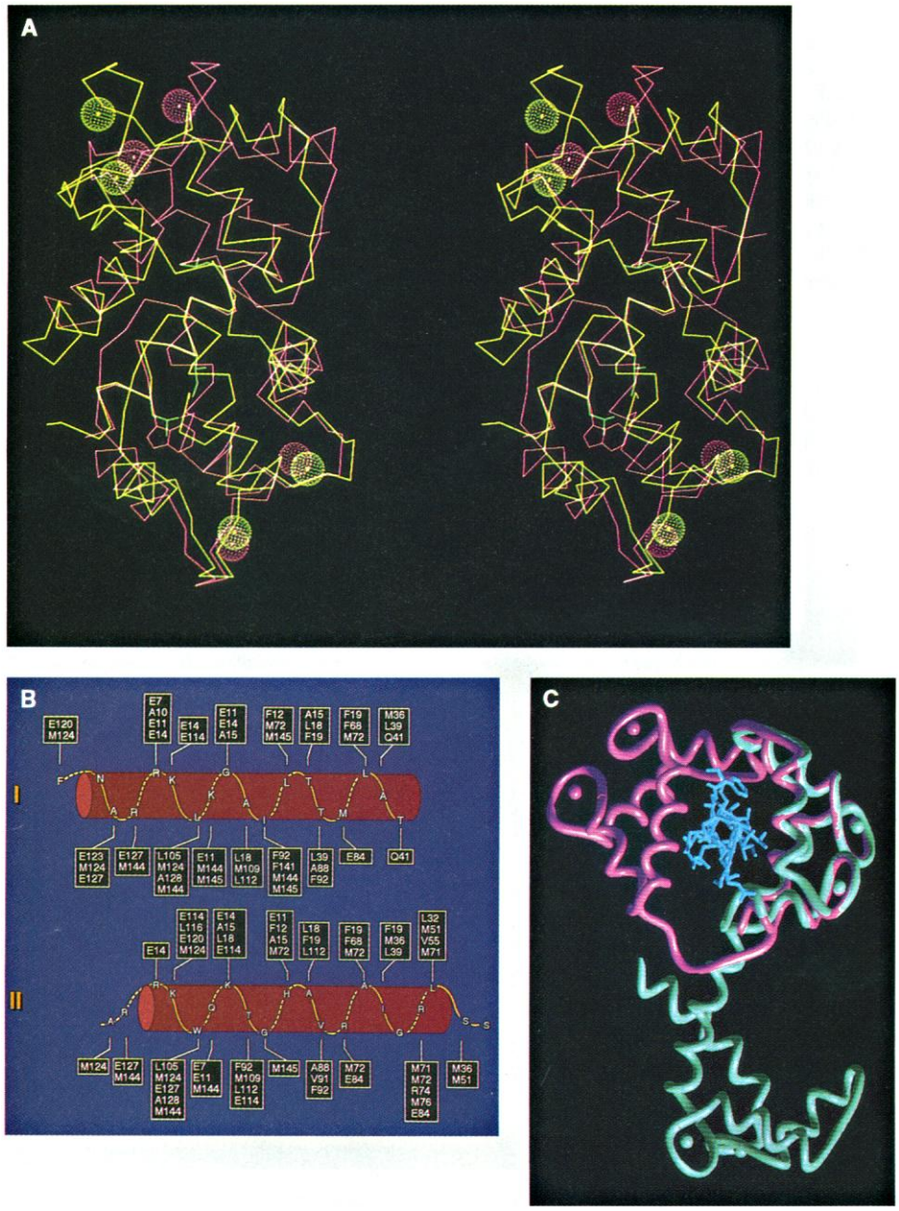

Fig. 3. Comparison of Ca^{2+}-CaM structures. (**A**) Stereo view of the Ca^{2+}-CaM-CaMKII peptide complex 2 Å structure (green) and the Ca^{2+}-CaM-smMLCK peptide 2.2 Å structure (magenta). Superimposed are the helical portions of the CaMKII peptide (with the side chains Leu^{299}, Ile^{303}, and Leu^{308}) and the smMLCK peptide with the side chains Trp^{800} and Leu^{813}. In the bound form, the CaMKII and smMLCK peptides (Fig. 1) are α-helical from residues 294 to 310 and 799 to 813, respectively. Portions of the central helix in the unbound Ca^{2+}-CaM complex are uncoiled in both complex structures, giving rise to four helices in both domains—I to IV for the NH_2-domain and V to VIII for the COOH-domain (*9*). (**B**) Schematic diagram of the interactions between the ordered residues of Ca^{2+}-CaM (enclosed in boxes) and those of the CaMKII peptide residues 290 to 314 (I) and the smMLCK peptide residues 293 to 310 (II) (*17*). Residues Arg^{797} and Ser^{814} of the smMLCK peptide are very close to being part of the helix (*9*). The interactions associated with the α-ammonium group of Ala^{796} of the smMLCK peptide are excluded. (**C**) Perspective model of the backbone structures of Ca^{2+}-CaM in the native unbound form (green) and in complex (magenta) with the CaMKII peptide (blue). The COOH-domain of CaM in both structures overlap. The four bound Ca^{2+} atoms in each structure are shown as spheres. The view is down the tunnel resulting from the two domains wrapping around the peptide with its NH_2-terminal end closest in view. This figure was generated with RIBBONS (*21*).

fluidity in the interconnecting helix (*15*). Thus, Ca^{2+} serves to organize and stabilize domain structure in a conformation that can bind the target, while the central helix remains flexible, an essential condition for target recognition. Target binding further stabilizes domain structure, which should and does increase Ca^{2+} affinity (*16*). We believe that the Ca^{2+} signal restricts the available conformational states of CaM to those that are most favorable to target recognition and activation. The modulation of the inherent plasticity of CaM by the different ligands is a key element of molecular recognition and the mechanism of signal transduction.

REFERENCES AND NOTES

1. C. B. Klee and T. C. Vanaman, *Adv. Protein Chem.* **35**, 213 (1982).
2. K. T. O'Neil and W. F. DeGrado, *Trends Biochem. Sci.* **15**, 59 (1990).
3. R. M. Hanley *et al.*, *Science* **237**, 293 (1987).
4. M. Katoaka *et al.*, *Proc. Natl. Acad. Sci. U.S.A.* **86**, 6944 (1989); D. B. Heidorn *et al.*, *Biochemistry* **28**, 6757 (1989); M. Ikura *et al.*, *ibid.* **30**, 9216 (1991); S. M. Roth *et al.*, *ibid.* **31**, 1443 (1992).
5. Y. S. Babu *et al.*, *Nature* **315**, 37 (1985).
6. Y. S. Babu, C. E. Bugg, W. J. Cook, *J. Mol. Biol.* **204**, 191 (1988).
7. R. Chattopadhyaya, W. E. Meador, A. R. Means, F. A. Quiocho, *ibid.* **228**, 1177 (1992).
8. M. Ikura *et al.*, *Science* **256**, 632 (1992).
9. W. E. Meador, A. R. Means, F. A. Quiocho, *ibid.* **257**, 1251 (1992).
10. I. Rayment *et al.*, *ibid.* **261**, 50 (1993).
11. W. E. Meador, A. R. Means, F. A. Quiocho, unpublished results.
12. T. Vorherr, M. Quadroni, J. Krebs, E. Carafoli, *Biochemistry* **31**, 8245 (1992).
13. The amphipathic helical CaMKII and smMLCK peptide segments portray two variations, with the overlapped hydrophobic residues Leu^{299} and Trp^{800} near the NH_2-terminal ends (Figs. 1 and 3, A and B). A third viable target sequence would be a hybrid of the two segments with an eight-residue sequence separating the two hydrophobic residues—one in an identical position as Leu^{813} of the smMLCK peptide near the COOH-terminal end and the other in an equivalent position to that of Ile^{303} of the CaMKII peptide, which is nestled in the COOH-domain. The presence of hydrophobic residues in all four key positions would represent the fourth and ideal target sequence. The wide hydrophobic cavity in both domains of Ca^{2+}-CaM (Figs. 2B and 3B), combined with adjustment of the domain geometry described in the text, makes it possible for Ca^{2+}-CaM to accommodate these variations.
14. S. H. Gellman, *Biochemistry* **30**, 6633 (1991).
15. The ease with which the central helix or expansion joint is deformable is indicated in the extent of disorder or the high thermal parameter of this region in the refined crystal structures. The expansion joint region in the complex with the CaMKII peptide is totally disordered, as is evident from the absence of electron density. Although the electron density of the expansion joint in the complex with the smMLCK peptide in the four independent molecules contained in the asymmetric unit was observed for the most part, this segment exhibited the highest averaged isotropic thermal *B* factor (*9*). In the native unbound 1.7 Å structure, this region of the central helix (from residues 73 to 83) has an averaged *B* factor 1.6 times greater than that of the entire molecule (*7*). The high thermal motion of the central helix was first noted in the 2.2 Å structure of native Ca^{2+}-CaM (*6*).
16. S. H. Seeholzer and A. J. Wand, *Biochemistry* **28**, 4011 (1989).
17. Abbreviations for the amino acid residues are: A, Ala; C, Cys; D, Asp; E, Glu; F, Phe; G, Gly; H, His; I, Ile; K, Lys; L, Leu; M, Met; N, Asn; P, Pro; Q, Gln; R, Arg; S, Ser; T, Thr; V, Val; W, Trp; and Y, Tyr.
18. A. R. Means, I. C. Bagchi, M. F. A. VanBerkum, C. D. Rasmussen, in *Cellular Calcium, A Practical Approach*, J. G. McCormack and P. H. Cobbold, Eds. (IRL, Oxford, 1991), pp. 205–245.
19. *X-PLOR, Version 3.1*, A. T. Brunger, Yale University.
20. J. S. Sack, *J. Mol. Graphics* **6**, 244 (1988).
21. M. C. Carson, *ibid.* **5**, 103 (1987).

22. Supported in part by an NIH grant to A.R.M. F.A.Q. is an investigator of the Howard Hughes Medical Institute. We thank T. Reynolds for assistance with Fig. 3B and D. Chin for purification of CaM. The coordinates for the Ca^{2+}-CaM-CaMKII peptide 2 Å structure and the Ca^{2+}-CaM-smMLCK peptide 2.2 Å structure have been deposited in the Protein Data Bank.

20 July 1993; accepted 19 October 1993

Restoration of HIV-Specific Cell-Mediated Immune Responses by Interleukin-12 in Vitro

Mario Clerici, Daniel R. Lucey, Jay A. Berzofsky, Ligia A. Pinto, Thomas A. Wynn, Stephen P. Blatt, Matthew J. Dolan, Craig W. Hendrix, Stanley F. Wolf, Gene M. Shearer*

Peripheral blood mononuclear cells (PBMCs) from many asymptomatic individuals infected with human immunodeficiency virus–type 1 (HIV) are unresponsive as measured by in vitro T cell proliferation and interleukin-2 (IL-2) production to influenza virus and synthetic peptides of HIV envelope (Env). Strong influenza virus– and Env-stimulated IL-2 responses and T cell proliferation were restored when cultures were stimulated in the presence of IL-12. Interferon-γ production by PBMCs from HIV seropositive (HIV^+) patients was also restored with IL-12. Furthermore, in vitro antigen-specific production of IL-2 and proliferation of PBMCs from HIV^- donors were suppressed by antibody to IL-12, but were not enhanced by addition of exogenous IL-12. Thus, IL-12 may be limiting in PBMCs from HIV^+ but not HIV^- individuals. These findings demonstrate that IL-12 can restore HIV-specific cell-mediated immunity in vitro in HIV-infected individuals and suggest a potential use of IL-12 in augmenting the diminished immunologic functions associated with HIV infection.

The recently discovered cytokine IL-12 has been reported to increase (i) natural killer cell and cytotoxic T lymphocyte (CTL) activity (*1*); (ii) T cell proliferation (*2*, *3*); and (iii) the production of interferon-γ (IFN-γ) (*4*). We previously demonstrated that the progression of HIV disease in HIV-infected (HIV^+) individuals is associated with a switch from a T helper 1 (T_H1)–like cytokine profile (high IL-2, low IL-4, and low IL-10 production) to a T_H2-like cytokine pattern (low IL-2, high IL-4, and high IL-10 production) (*5*, *6*). This change in cytokine profile is predictive of a decline in the number of peripheral blood $CD4^+$ T cells (*7*), as well as of the time until diagnosis of acquired immunodeficiency syndrome (AIDS) and time to death (*7*). We recently demonstrated that IL-4 and IL-10 antibodies can reverse the T_H1-to-T_H2 switch in vitro and restore in vitro the ability of the PBMCs of HIV^+ individuals to produce IL-2 (*6*). IL-12 can bypass the inhibitory effect of IL-10 on the induction of a T_H1-like function (*4*). Therefore, on the basis of the above findings we asked whether the defective T_H1-like cell-mediated responses of PBMCs from HIV^+ individuals could also be reconstituted in vitro by IL-12.

The PBMCs of 40 HIV^+ individuals that were unable to produce IL-2 in response to five synthetic peptides corresponding to antigenic regions of the envelope (Env) of HIV-1 (*8*) in vitro were stimulated with Env in the presence of IL-12 (*9*). The data obtained from three representative individuals are shown in Fig. 1A (panels a through c), along with the response generated by PBMCs from an uninfected, healthy control donor (panel d). Cultures from all three of the HIV^+ individuals responded strongly to Env only when IL-12 was added. In contrast, IL-12 did not elevate above the background the IL-2 response to Env of the HIV^- culture or induce IL-2 production by HIV^+ cultures in

M. Clerici, D. R. Lucey, L. A. Pinto, G. M. Shearer, Experimental Immunology Branch, National Cancer Institute (NCI), National Institutes of Health (NIH), Bethesda, MD 20892.
J. A. Berzofsky, Metabolism Branch, NCI, NIH, Bethesda, MD 20892.
T. A. Wynn, Laboratory of Parasitic Diseases, National Institute of Allergy and Infectious Diseases, NCI, Bethesda, MD 20892.
S. P. Blatt, M. J. Dolan, C. W. Hendrix, HIV Unit, Wilford Hall Medical Center, Lackland Air Force Base, TX 78236.
S. F. Wolf, Genetics Institute Inc., Cambridge, MA 02140.

*To whom correspondence should be addressed at Experimental Immunology Branch, NCI, Building 10, Room 4B-17, NIH, Bethesda, MD 20892.